ADVANCED BIOSYSTEMS
www.adv-biosys.com

Mechanical Regulation of Endocytosis: New Insights and Recent Advances

*Jophin G. Joseph and Allen P. Liu**

Endocytosis is a mechanosensitive process. It involves remodeling of the plasma membrane from a flat shape to a budded morphology, often at the sub-micrometer scale. This remodeling process is energy-intensive and is influenced by mechanical factors such as membrane tension, membrane rigidity, and physical properties of cargo and extracellular surroundings. The cellular responses to a variety of mechanical factors by distinct endocytic pathways are important for cells to counteract rapid and extreme disruptions in the mechanohomeostasis of cells. Recent advances in microscopy and mechanical manipulation at the cellular scale have led to new discoveries of mechanoregulation of endocytosis by the aforementioned factors. While factors such as membrane tension and membrane rigidity are generally shown to inhibit endocytosis, other mechanical stimuli have complex relationships with endocytic pathways. At this juncture, it is now possible to utilize experimental techniques to interrogate theoretical predictions on mechanoregulation of endocytosis in cells and even living organisms.

1. Introduction

Endocytosis involves transport of nutrients, macromolecules, and pathogens across the plasma membrane by forming membrane invaginations and subsequently internalizing the cargo in a membrane-enclosed vesicle. Endocytosis plays a role in various cellular processes including signal transduction, immune response, cell division, and cell migration.[1–3] Endocytosis is often exploited by toxins and pathogens like bacteria and viruses to gain entry into a cell,[4] but cells also rely on endocytosis to neutralize pathogens.[5] Eukaryotic cells have evolved multiple pathways of endocytosis to internalize cargos of different types and sizes (**Figure 1**). A critical step of several endocytic pathways is the formation of a budded membrane invagination by sculpting the plasma membrane. Different endocytosis pathways utilize different protein complexes to generate, stabilize, and internalize membrane buds.[6] Activity of curvature generating processes including imposition of intrinsic protein curvature onto the membrane (BAR proteins), insertion of amphipathic helix (E/ANTH domain proteins), steric repulsion by protein crowding, and polymerization of actin networks, is required for bud formation.[7] The membrane invaginations are stabilized by scaffolding proteins like clathrin, caveolin, and by activity of actin cytoskeleton.[1,6,8,9] Proteins like dynamin aid the fission of membrane buds from the lipid bilayer.[6,9] Mechanical factors like bending rigidity of the lipid bilayer, membrane tension, stiffness of the extracellular matrix (ECM), shape, size, and stiffness of the cargo can affect the effectiveness of the membrane remodeling process.[5,6,9,10] Membrane rigidity and membrane tension act as limit agents against the spontaneous membrane curvature generation by creating an energy barrier for membrane deformation. Furthermore, the aforementioned mechanical factors also regulate the fission of membrane invaginations to create endocytic vesicles.[1] Quantifying the effects of mechanical factors on membrane curvature generation, curvature stabilization, and membrane scission is critical for understanding how these factors influence the overall trafficking and regulatory role of endocytosis. Since nanoparticle-based drug delivery systems target different endocytic pathways in cells, understanding the interplay between mechanical factors and endocytosis can aid in better designs of these drug carrier systems.[10]

Most endocytic events (<100 nm) occur below the diffraction limit of light. Hence, studying the morphological development of endocytic structures using conventional optical microscopy does not offer sufficient spatial resolution for in-depth dissection of their assembly. Further, robust techniques to control mechanical properties of cells were largely inaccessible until the last decade. Hence, our understanding of mechanoregulation of endocytosis primarily came from molecular simulations and in vitro reconstitution of endocytic proteins on vesicles. Recent developments, improvements, and

J. G. Joseph, Prof. A. P. Liu
Department of Mechanical Engineering
University of Michigan
Ann Arbor, MI 48109, USA
E-mail: allenliu@umich.edu
Prof. A. P. Liu
Department of Biomedical Engineering
University of Michigan
Ann Arbor, MI 48109, USA
Prof. A. P. Liu
Cellular and Molecular Biology Program
University of Michigan
Ann Arbor, MI 48109, USA
Prof. A. P. Liu
Department of Biophysics
University of Michigan
Ann Arbor, MI 48109, USA
The ORCID identification number(s) for the author(s) of this article can be found under https://doi.org/10.1002/adbi.201900278.

DOI: 10.1002/adbi.201900278

implementation of advanced microscopy techniques like stochastic optical reconstruction microscopy (STORM), structured-illumination microscopy (SIM), polarized total internal reflection fluorescence (TIRF) microscopy, and correlative light and electron microscopy (CLEM) have enabled researchers to look beyond diffraction limit into the protein architecture of endocytic structures while they are budding.[11] Robust techniques to mechanically manipulate cells, which are compatible with high-resolution microscopy, like cell stretchers, microcontact printing, stiffness tunable hydrogels, and micropillar arrays, also gained progress in the last decade.[12–15] Automated algorithms for detecting and tracking endocytic events coupled with these sophisticated imaging techniques have enabled visualization of endocytosis in living organisms.[16–18]

Simultaneous utilization of subdiffraction-limited microscopy and robust techniques to mechanically manipulate cells has provided us with important insights into how endocytic protein complexes respond to mechanical stimuli. In recent years, these sophisticated techniques have spurred interests in experimentally validating theoretical and computational predictions on the mechanobiology of endocytosis. At the same time, these advances have reignited once settled controversies about endocytosis. Newer studies utilizing aforementioned techniques have called into question whether membrane bud formation in clathrin-mediated endocytosis (CME) occur primarily via a constant curvature mechanism, or the newly emerging flat-to-dome mechanism.[12,19] Recent findings have also strengthened nonspecific membrane bending hypotheses like steric crowding as an alternative to protein-specific mechanisms such as amphipathic helix insertion.[20,21]

In this review, we will survey recent studies that provided insights into mechanoregulation of endocytosis. We will consider the mechanoregulation of endocytosis pathways including CME, caveolae-mediated endocytosis, caveolae and clathrin-independent endocytosis (CIE), macropinocytosis, and phagocytosis (Figure 1). We further analyze mechanoregulation of individual steps of CME, one of the prominent endocytic pathways. We specifically focus on several key mechanical factors, including i) membrane tension, ii) membrane rigidity, iii) physical properties of extracellular surroundings, and iv) physical properties of cargo (**Figure 2**). Competing hypotheses on mechanoregulation of membrane sculpting will be scrutinized to provide a progress report on the present state of understanding on how mechanical cues control endocytosis.

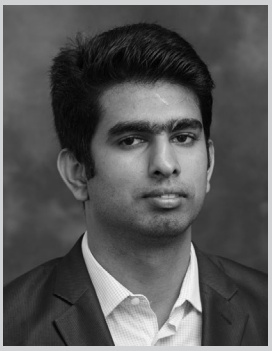

Jophin G. Joseph received his B.Tech. (Hons) in chemical engineering (2016) from the Indian Institute of Technology, Hyderabad. He was an S.N. Bose exchange student in the University of Michigan in the summer of 2014, where he worked on developing microfluidic chips for leukemia diagnosis. In 2016, he joined the University of Michigan, Department of Mechanical Engineering as a Ph.D. student under the guidance of Dr. Allen Liu. He currently works on the mechanoregulation of clathrin-mediated endocytosis. His research interests include mechanobiology, intracellular trafficking, super-resolution microscopy, and microfluidics.

Allen P. Liu is Associate Professor in the Department of Mechanical Engineering at the University of Michigan. He earned a bachelor's degree in biochemistry at the University of British Columbia. In 2007, he earned a doctorate in biophysics at UC Berkeley, working in the field of in vitro reconstitution of membrane and cytoskeleton interaction. From there, he went on to do a postdoctoral fellowship at The Scripps Research Institute in quantitative cell biology of clathrin-mediated endocytosis. His group's research interests are in mechanobiology of biological membranes.

2. Mechanical Factors Regulating Endocytosis

It is well appreciated that several mechanical factors regulate endocytosis. In this section, we will provide an overview of different mechanical factors, considering the properties of membrane, extracellular interaction, and cargo.

2.1. Membrane Tension

The plasma membrane of cells is under tension as a result of the in-plane tension in the lipid bilayer due to intracellular hydrostatic pressure and out-of-plane tension due to membrane–cytoskeleton adhesion.[22] Membrane–cytoskeleton adhesion enables the cytoskeleton to exert forces onto the plasma membrane. Hence, in-plane and cytoskeletal components of membrane tension are interdependent[23] and together they play a major role in regulating endocytosis.[18,22,24,25] Cellular processes associated with the creation of tension gradients can lead to spatiotemporal heterogeneity of endocytosis.[8,16] Membrane tension affects the rate of nucleation and lifetime of endocytic events in different pathways by inhibiting curvature formation and membrane scission.[8,12,23,26] An acute drop in membrane tension is also associated with initiation of ultrafast endocytosis and formation of clustered endocytic structures.[27,28] Increased membrane tension inhibits the transition of membrane invaginations from an open (U shape) to a close (Ω) topology (Figure 2a).[8,29,30] An increase in plasma membrane tension has been associated with stalling of endocytic structures in the membrane[8,12,31] and an alteration of the morphology

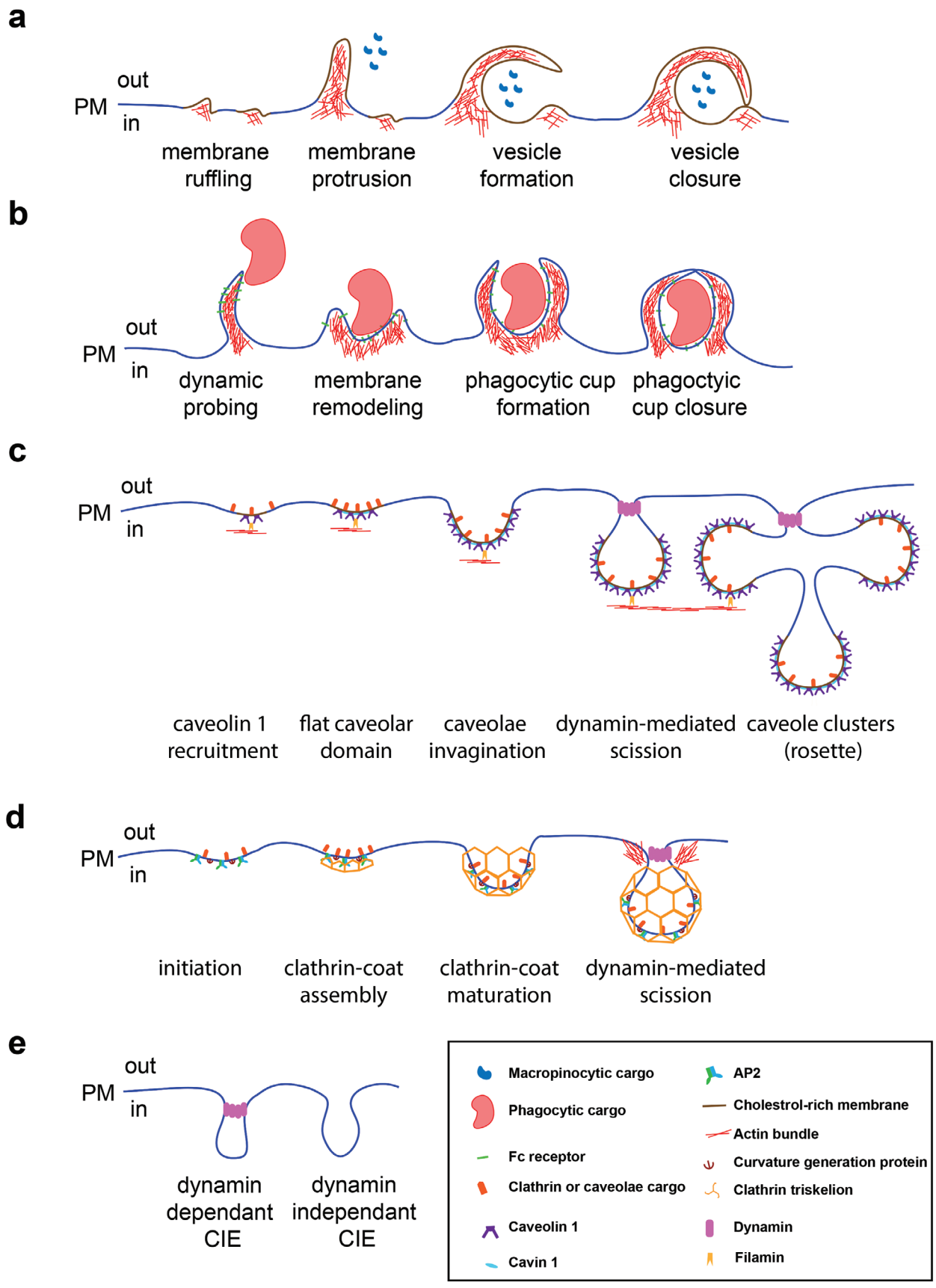

and size of endocytic pits.[25,28,32–34] Coarse-grained simulations show that at high membrane tensions (0.2 pN nm^{-1}), the assembly of coat proteins may not be sufficient to induce an open to a close bud morphology transition critical for endocytosis.[29] Whereas, at low membrane tensions (0.002 pN nm^{-1}), the membrane evolves smoothly from a flat to budded morphology with increasing coat area of endocytic proteins.[29] Activities of actin cytoskeleton and membrane curvature generation proteins are necessary to rescue endocytosis at high tension.[8,29,35] Thus, membrane tension and coat area of endocytic proteins control the shape of membrane invaginations.[29,35] For instance, membrane tubulation can be induced by increasing protein coverage at constant membrane tension or by decreasing membrane tension at constant coverage.[35]

In the last decade, we have gained a better understanding of the role membrane tension plays in several classical pathways of endocytosis (e.g., CME and phagocytosis).[22,36] At the same time, newer studies are putting much more emphasis on CIE pathways and their coupling with exocytosis as a major response mechanism against membrane tension variations.[6,37] We expect such studies to uncover deeper insights into how cells cope with acute variation in membrane tension (e.g., muscle cells), perhaps by coupling fast endocytosis with exocytosis to prevent membrane damage.

2.2. Membrane Rigidity

Bending rigidity of the plasma membrane determines the resistance of the lipid bilayer to bending,[38,39] and it can govern endocytosis (Figure 2b). Bending rigidity of the bilayer strongly depends on the composition of the membrane.[39] Reduction of bending rigidity of the membrane by incorporation of polyunsaturated phospholipids was shown to increase endocytic activity.[40] Insertion of amphipathic helix (an alpha helix) of a protein into membranes initiates membrane budding by altering membrane rigidity.[41,42] Alpha helix insertion rigidifies the membrane and induces spontaneous curvature in a lipid bilayer. However, as the insertion depth increases, the membrane rigidity reduces after reaching a maximum.[42] Concurrently, spontaneous curvature changes from positive to negative.[42] Once the endocytic coats are formed, the increased rigidity imparted by the coat proteins stabilizes invaginations.[38,43] Membrane bending simulations showed that bending rigidity mediates the smooth transition between open (U-shaped) to closed (Ω-shaped) endocytic pits by avoiding snap-through instability.[29] The snap-through instability occurs when a small change in endocytic coat area causes the hemispherical bud to abruptly close to a Ω-shaped morphology.[29,30] Membrane rigidity also controls the ease of scission of endocytic vesicles from the plasma membrane.[44,45] An increase in membrane rigidity delays or inhibits vesicle scission by increasing the elastic energy barrier for dynamin-mediated membrane fission.[45]

2.3. Physical Confinement of Cells and Mechanical Properties of Extracellular Matrix

Endocytosis pathways play important roles in mediating the interaction between cells and the ECM. Physical confinement of cells and properties of ECM like stiffness have been shown to regulate endocytosis[5,46] (Figure 2c). Cells spread on large adhesive islands showed a reduction in clathrin-mediated endocytic and phagocytic activity.[25,47] Changes in ECM stiffness, due to infection or other disease conditions, can initiate phagocytosis response in macrophages.[48,49] An increase in matrix stiffness enhances vascular endothelial growth factor receptor VEGFR-2 internalization, signaling, and proliferation of tumor-like phenotype in endothelial cells.[50,51] Endocytosis of integrin $\beta 1$ in bone marrow mesenchymal stem cells on collagen I-coated substrates promotes cell differentiation to a neuronal lineage.[52] Thus, cells may utilize endocytic pathways as a mechanosensitive conduit for sensing and responding to changes in ECM. Strong adhesion to ECM may also affect the endocytic uptake.[53–55] Cells adhered on fibronectin show reduced rate of CME compared to cells attached on BSA-coated coverslips. The substrate adhesion-induced inhibition of CME may be due to the direct linkage of CCPs with ECM-bound integrin $\beta 1$.[53] Earlier EM-based studies have shown that strong adhesion of the plasma membrane to the substrate promotes the formation of flat clathrin lattices.[54,55] Physical confinement of cells and increase in ECM stiffness could downregulate membrane remodeling on the adherent face of cells, which is necessary for endocytosis.

Figure 1. Progression of endocytic pathways. a) Clathrin-mediated endocytosis is initiated by the recruitment of adaptor protein AP2 and membrane bending proteins like E/ANTH domain proteins and F-BAR proteins to the membrane. Clathrin triskelia bind to AP2 and polymerize to form clathrin coats with hexagonal and/or pentagonal faces. Whether the coat is formed before or after the start of membrane bending is still contested. Once the coated pit matures to a hemispherical shape, it is transitioned to an Ω shape (with the help of actin at high tension), enabling dynamin-mediated scission.[1] b) Caveolae-mediated endocytosis is initiated at cholesterol-rich membrane sites by the recruitment of caveolin-1. Caveolae associated proteins like cavin-1 enables the polymerization of caveolin-1, leading to the formation of caveolae. Caveolae are linked with actin stress fibers through filamin A. Membrane tension and stress fiber activity plays a role in the transformation of caveolae into a flask shape, enabling dynamin-mediated scission. High membrane tension and excess stress fiber linkage can flatten caveolae, whereas a sudden drop in membrane tension and stress fiber disruption lead to formation of caveolae clusters known as rosettes.[28] c) Clathrin-independent endocytosis pathways exist in two types. Pathways that utilize dynamin for membrane scission and pathways that do not utilize dynamin for membrane scission.[6] d) Macropinocytosis is initiated by actin polymerization near the membrane in response to receptor activation, leading to membrane ruffling. Membrane protrusions are formed from the ruffles, which may fold back to the plasma membrane to form vesicles. The fusion of folded membrane protrusions to basal membrane creates macropinosomes, encapsulating extracellular fluid and other cargo.[4] e) Phagocytosis is initiated by binding specialized receptors on the cell membranes to target particles. Phagocytic cell-like macrophages actively probe for pathogens by forming pseudopodial extensions. Once the particle for internalization is located, the plasma membrane is remodeled by actin polymerization to wrap around the particle to form a phagocytic cup. The phagocytic cup is closed by the depolymerization of actin at the base of the cup, forming a membrane-bound phagosome.[4]

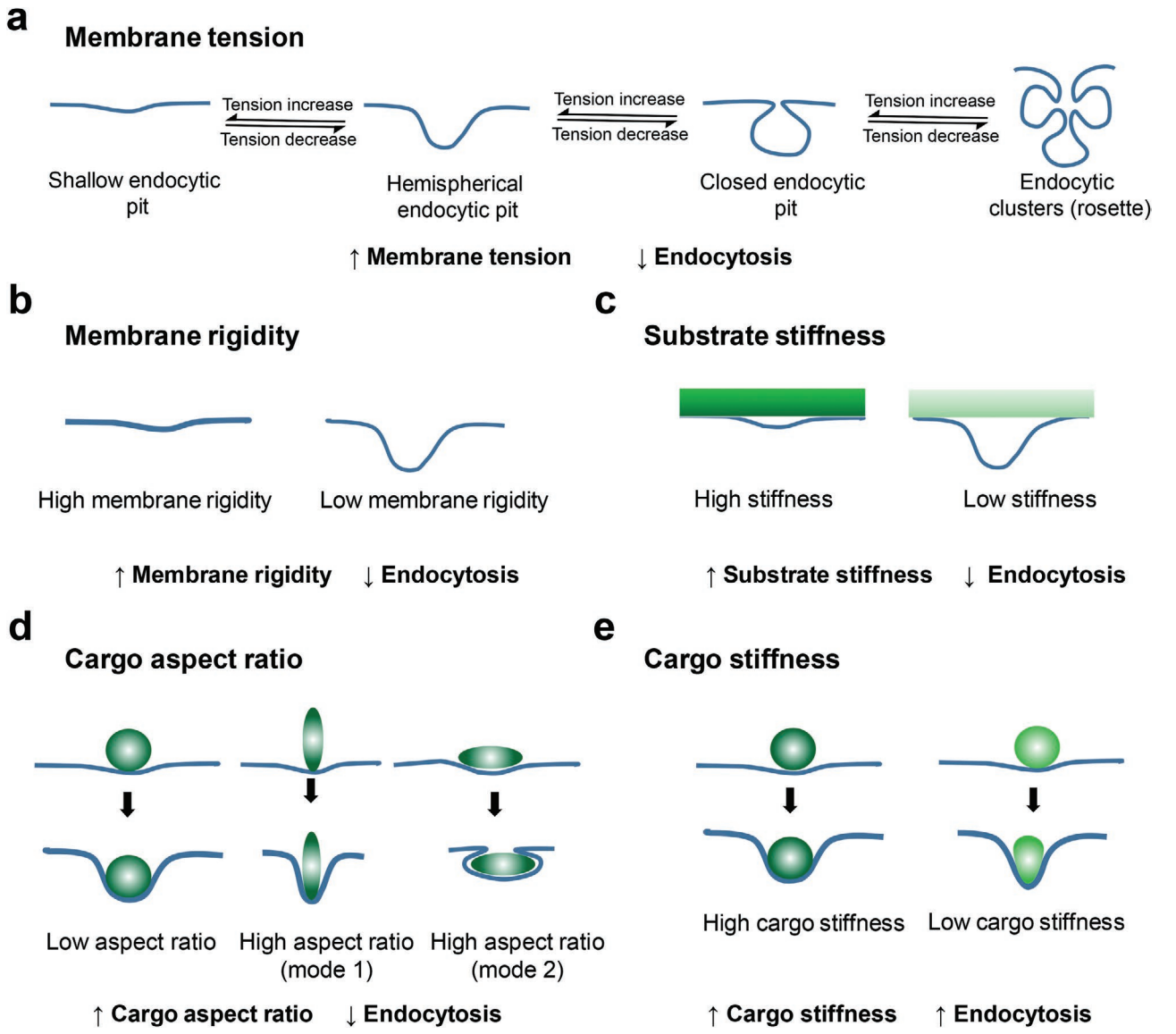

Figure 2. Effect of mechanical stimuli on endocytosis. a) Membrane bending requires work done against membrane tension. Transition of membrane from flat-to-dome and dome-to-Ω shape is mediated by recruitment of proteins that provide energy to overcome the membrane tension energy barrier.[7,81] An acute increase in membrane tension leads to the flattening of membrane buds and an acute reduction in membrane tension can lead to the formation of endocytic clusters (in caveolae-mediated endocytosis).[28,113] b) Bending rigidity of plasma membrane defines its resistance to undergo bending. Bending rigidity of the plasma membrane depends on the composition of membrane and protein recruitment to the plasma membrane alters membrane rigidity.[29,30] c) Extracellular substrate stiffness regulates the ability of membrane to undergo deformation. Membrane adhered to a stiffer substrate is less deformable compared to the ones adhered on a softer substrate.[32] d) Cargos with a low aspect ratio (spherical shape) can be internalized easily by endocytic pathways due to the ease of membrane wrapping around them. Cargos with a high aspect ratio can inhibit endocytosis by impeding membrane wrapping. High aspect ratio cargos can be internalized by membrane wrapping from its pole (mode 1) or membrane wrapping along its shallow edge (mode 2). Cells prefer pole-based internalization for high aspect ratio cargos.[10,61] e) Stiffer cargo is internalized via wrapping the cellular membrane without deforming the particle. Softer cargo undergoes large deformation during internalization causing changes in aspect ratio thereby increasing the energy barrier for full wrapping.[10,64]

Increased substrate stiffness can inhibit or stall endocytosis on the adherent face of a cell.[32] Cells also respond to different substrate stiffness by preferentially up- or downregulating specific endocytic pathways. Cellular uptake of nanoparticles by bovine aortic endothelial cells on a stiff substrate resulted in a higher total cellular uptake on a per cell basis, but a lower uptake per unit membrane area.[56] Cells cultured on softer hydrogel substrate exhibited reduced CME of transferrin without affecting the rate of CIE of cholera toxin subunit B.[46] Until recently, researchers have largely ignored the effect of physical microenvironment on endocytic pathways like phagocytosis.[5] This gap of knowledge was due to the fact that traditional cell-based studies are performed on 2D petri dishes. Wider usage of 3D and 2D cell culture systems with tunable

stiffness that are amenable for high-resolution microscopy will hopefully bridge this knowledge gap. It is not yet clear whether an increase in ECM stiffness or physical confinement of cells have an inhibitory effect on all endocytic pathways. Furthermore, we have barely scratched the surface on the crosstalk between ECM properties and endocytic cargo properties, and how they regulate the endocytic machinery. Future works need to address the combinatorial effects of multiple mechanical stimuli on endocytosis.

2.4. Physical Properties of Cargo: Shape, Aspect Ratio, and Stiffness

Endocytosis is the primary mode of entry for particulate matter like nanoparticles, viruses, and bacteria into the cells. The physical properties of these cargos can often determine the type of endocytic pathway used and the rate of uptake.[57] The endocytic pathway for nanoparticles depends on the size, aspect ratio, and stiffness.[10] Hydrogel-based nanoparticles with a large bulk modulus (3000 kPa) were internalized at a higher rate by epithelial tumor cells and brain endothelial cells, compared to internalization of softer particles.[58] The phagocytic rate by J774 macrophages is also higher for stiff particles compared to softer ones.[58] Spherical nanoparticles with a 25 nm radius and made with different materials (gold, silica, and single-walled nanotubes) have an optimum endocytic uptake.[10,59,60] Nanoparticles and other cargos with higher aspect ratio show reduction in uptake compared to low aspect ratio ones. It is thought that an increase in aspect ratio impedes effective membrane wrapping needed for endocytic entry. However, when high aspect ratio nanoparticles become oriented with the major axis being perpendicular to the membrane, the nanoparticles may enter the cell by tip entry (Figure 2d).[10,56,61] Interestingly, pathogens like *Escherichia coli* and fungi form high aspect ratio filaments during infection, and this could cleverly inhibit phagocytosis and help pathogens evade an immune response.[62,63] Molecular dynamic simulations have shown that softer nanoparticles may increase the energy barrier for effective membrane wrapping due to an increase in curvature of the leading edge of particle during internalization (Figure 2e).[10,64] Interestingly, this deformation of nanoparticles during internalization negatively regulates uptake.[64] For instance, macrophages prefer uptaking stiff microgels via macropinocytosis and softer gels via phagocytosis.[65] This may be due to the extensive membrane remodeling capability of the phagocytosis pathway. Optimizing the physical properties of nanoparticles and other drug delivery vehicles to improve cellular entry via endocytosis—a concept known as mechanotargeting—in combination with chemotargeting may advance the specificity of cellular targeting.[66–68]

In the following sections, we will review key understanding of how various physical and mechanical properties of the plasma membrane and cargo regulate specific endocytic pathways.

3. Clathrin-Mediated Endocytosis

CME involves internalization of cargo by packaging it in 60–120 nm sized clathrin-coated vesicles.[1] CME is a well-studied endocytic pathway, fundamental to nutrient uptake, neurotransmission, signal transduction, and intercellular communication.[1,4,69] CME, with clathrin-coated pits (CCPs) as the fundamental functional units, is a multistep process involving extensive sculpting and reorganization of the plasma membrane. Initiation of CME is triggered by the recruitment of adaptor protein complex AP2 and membrane bending BAR domain and E/ANTH domain proteins.[70,71] The clathrin coat is assembled at the sites of adaptor protein nucleation. Concurrent with cargo recruitment, a CCP matures into a dome-shaped invagination, which is subsequently reorganized to a Ω-shaped pit and separated from the plasma membrane to form a clathrin-coated vesicle. The membrane reorganization in CME is regulated by mechanical factors like membrane tension, membrane rigidity, and stiffness of the ECM and cargo.[7,31] In the section below, we will examine how different stages of CME, through a CCP's lifecycle from initiation to scission, is modulated by mechanical stimuli.

3.1. Initiation

The initiation of CME is marked by the arrival of early endocytic adaptor proteins like AP2.[4] Although initiation events are generally considered stochastic,[72] "hot spots" for CCP initiation exist at specific regions of cells,[73] which can be based on the presence of specific lipid or cargo proteins.[1] FCHo1/2 proteins containing a F-BAR domain create and sustain membrane curvature for AP2 nucleation.[70,71] Sustained presence of FCHo proteins in the membrane have been shown to lead to formation of CCP hotspots.[70] Initiator proteins including FCHo1/2, Eps15, epsin, and intersectin form nucleating complex promoting CCP initiation and cargo binding.[70,71,74] Existence of multiple initiator proteins may suggest parallel and redundant nucleating activities by these proteins (e.g., FCHo1 and Eps15).[75] However, whether this redundancy acts as a failsafe switch to sustain CME under different mechanical stimuli needs to be further studied. Mechanical factors like area of confinement, local membrane tension, and polarity of a cell may play a role in the selective initiation of CME at specific membrane sites.[8,25,76,77] Endocytic proteins like AP2, epsin 1, and amphiphysin 1 show preferential recruitment to regions of pre-existing sub-micrometer curvature. Consistent with this, precurved membranes show increased rate of endocytic nucleation events.[78] In this context, an increase in membrane tension correlates with a reduction in CME initiation density.[31] CME nucleation proceeds only after the recruitment of membrane curving protein above a critical density, above which the membrane transitions from a flat-to-dome morphology, and this critical density is a function of membrane tension.[30,35] Coarse-grained molecular dynamic simulations show that membrane tension controls the assembly of curvature generating BAR domain-containing proteins. Elevated tension can alter the geometry of membrane-associated BAR protein assembly by inhibiting protein oligomerization, and the interaction between N-BAR domain and the membrane.[79] Local reduction in membrane tension by myosin-based contraction can accelerate the recruitment of BAR proteins at the leading edge of a polarized cell.[80]

Membrane bending proteins can alter the mechanical property of the membrane to achieve membrane curvature.[81] Purified ENTH domain binding to giant unilamellar vesicles (GUVs) causes a considerable reduction in area compressibility modulus and the bending rigidity of the membrane.[41] The insertion of helix-0 of ENTH domain into membrane tubulates membrane at low tensions and softens the bilayer at higher tensions.[41] Helix insertion reduces the energetic cost of membrane bending and makes tubule formation energetically less costly.[41,82] Consistent with this, osmotic pressure-induced tension enhances the hydrophobic insertion of N-BAR domain of amphiphysin into membrane.[83] This may be due to the increase in density of lipid packing defects, which aids in helix insertion of BAR proteins.[84,85] Further, spontaneous membrane bud formation aided by protein crowding by intrinsically disordered proteins like epsin and AP180 is also controlled by global membrane tension, which balances lipid–protein binding energy and membrane free energy.[86]

3.2. Coat Assembly

Clathrin triskelia are recruited directly to adaptor protein nucleation sites to form cage-like clathrin coat.[4] Clathrin polymerization is necessary for the stabilization of the membrane invaginations. There exist two competing hypotheses for clathrin scaffolding mechanism. The first model, the constant curvature model, considers the direct polymerization of clathrin coat to curved membrane as the pit increases in size (**Figure 3**a(top),b). A second model, the constant area model, considers clathrin assembly to occur on flat membrane and after the critical density of clathrin coat is reached, the flat assembly reorganizes into a spherical coat while maintaining a constant clathrin coat area (Figure 3a(bottom),b).

The assembly and formation of the coat is regulated by membrane tension and rigidity.[7,22] Membrane tension has an inhibitory effect on clathrin coat polymerization, coat size, and shape.[25,34] The shape stability curve of membrane invaginations shows the existence of multiple invagination topologies mediated by membrane tension and protein density[34] (Figure 3c). An increase in membrane tension results in premature disassembly of clathrin coat.[25,35] Increasing membrane rigidity also inhibits clathrin coat formation.[34,35] This is consistent with the early finding that the rate of endocytosis is slower on the apical side of an epithelial layer where the membrane rigidity is elevated.[87] Membrane curvature generation proteins like epsin enable coat formation under higher tensions and rigidity,[29,34] but the precise mechanism of how epsin achieves this remains unknown. While small, curved, and pit-like structures with nonhexagonal faces are found on the apical membrane, flat, flake-like clathrin structures, which are slowly internalized with the help of actin, are predominantly found on the basal surface of fibroblasts adhered to a solid substrate, in addition to pits.[88] Coarse-grained modeling shows that higher tension stabilizes large, flat clathrin plaques, whereas lower tension leads to smaller budded structures.[89] An increase in substrate rigidity causes the formation of stalled and flat clathrin-coated structures that are mediated by $\alpha v\beta 5$ integrin.[32] Although in vitro biochemical data on clathrin coat polymerization have favored the constant curvature model,[1] the observation of flat clathrin lattices have challenged the canonical constant curvature model. Recent studies based on correlative fluorescence and electron microscopy have shown evidence for the existence of the constant area model (model 2) for clathrin coat formation.[12,19,90] Quantification of membrane curvature by polarized TIRF during clathrin assembly shows the presence of both modes of coat curvature generation (constant curvature model and constant area model) in the same cell[19] (Figure 3b). Constant area model of coat formation by flat-to-dome transition is heavily regulated by clathrin-adaptor ratio and membrane tension. Osmotic shock-induced tension increase inhibits the transition of flat-to-dome coated structures[12] (Figure 3d,e). It is plausible that factors determining the mode of clathrin coat assembly, like distribution of membrane bending proteins,[91] lateral membrane tension,[12,34] local actin polymerization,[8,92] and cargo binding[93,94] vary locally in the plasma membrane, leading to the presence of both modes of assembly in cells.

3.3. Maturation and Scission

The clathrin coat assembly leads to the formation of hemispherical CCPs. Transition of hemispherical domes (U-shaped) to closed (Ω-shaped) pits is necessary for the internalization of cargo molecules. Membrane scission proceeds by assembling dynamin into tight oligomers of initial radius of 10 nm around the neck of a CCP to constrict the neck.[1] Coarse-grained simulations show that at physiologically relevant membrane tension (0.02 pN nm^{-1}), the transition from an open to a closed bud occurs spontaneously through a snap-through instability.[29,30] At high tension, increasing the coat rigidity and the force from actin polymerization around CCPs together ensure CCPs go through a smooth transition from an open to closed bud morphology without snap-through instability[29] (**Figure 4**a–d). This is consistent with a previous study where disrupting actin cytoskeleton by Jasplakinolide caused stalling of CCPs in cells under hypo-osmotic shock.[8] The transition of hemispherical bud to Ω-shaped bud exists over a range of membrane tension, and it is driven by BAR domain proteins and actin cytoskeleton (Figure 4e).[30] Super-resolution imaging has enabled the visualization of actin-aided transition of CCPs from open to close buds in yeast cells (Figure 4f–h).[95] BAR domain proteins also facilitate membrane scission of CCPs. BAR protein scaffold imposes a frictional force on the neck of the membrane invagination, while an external force provided by actin assembly can pull to elongate the invagination. Although CME does not rely on dynamin to mediate membrane scission in yeast, a similar principle applies where the BAR domain of Rvs161/167p stabilizes the neck and induces friction to mediate scission of the membrane (Figure 4i).[96]

4. Caveolae-Mediated Endocytosis

Caveolae-mediated endocytosis uses membrane proteins caveolins (e.g., Cav-1) and cavins to create 50–60 nm sized, sphingolipid and cholesterol-rich, flask-shaped plasma membrane

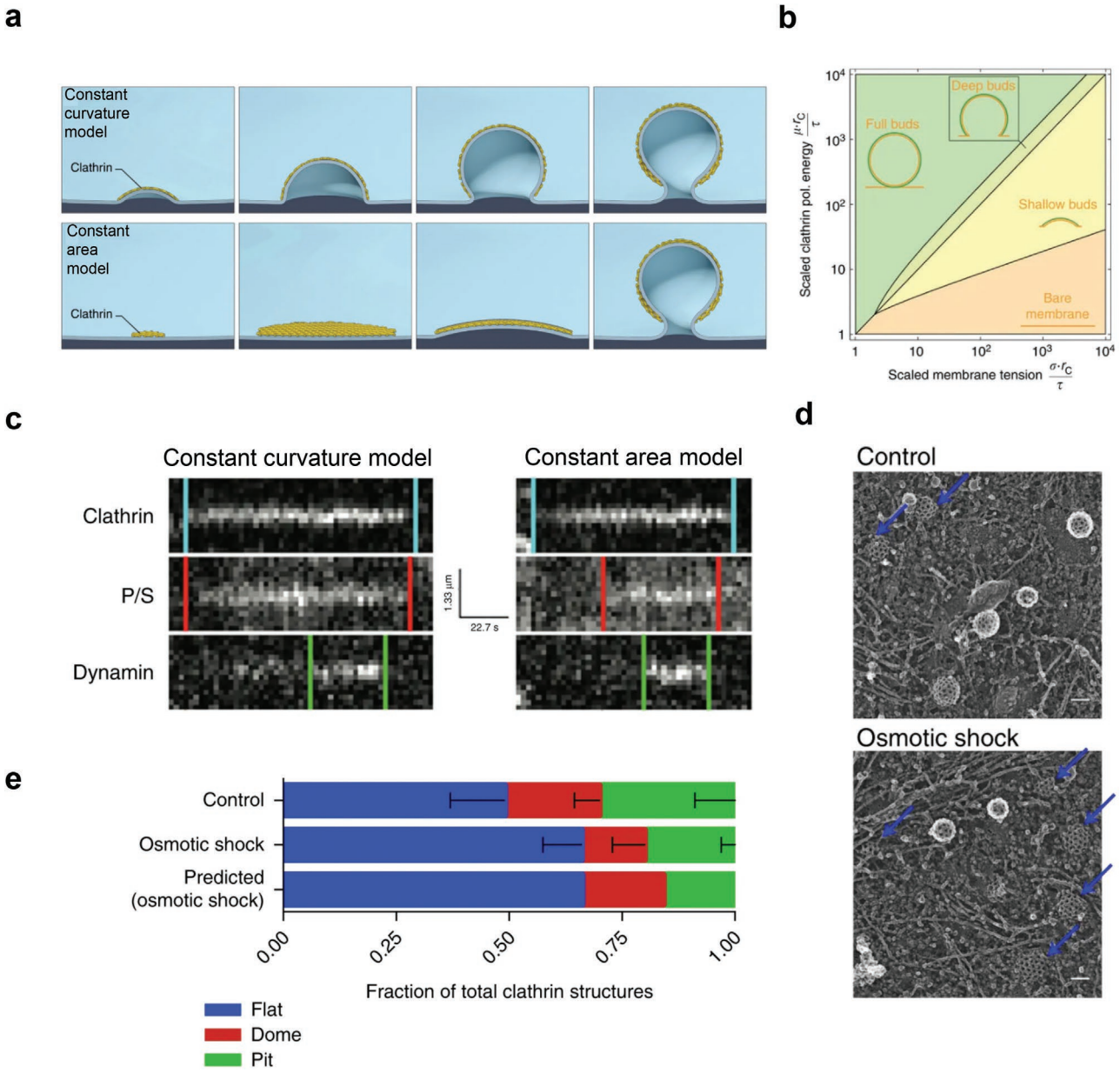

Figure 3. Clathrin bud formation under different tensions. a) Membrane bending model for clathrin-mediated endocytosis (CME). Constant curvature model (top panel), where membrane bending proceeds with a constant radius of curvature with continuous addition and polymerization of clathrin triskelion. Constant area model (bottom panel), where clathrin triskelion polymerizes into a flat coat then remodels into a coated pit. Reproduced under the terms of the CC BY 4.0 license.[19] Copyright 2018, The Authors, published by Springer Nature. b) Distinct mode of membrane bending observed in cells via polarized-TIRF. Constant curvature model for membrane bending observed by pol-TIRF (left panel). Clathrin and P/S signals proceed together indicating synchrony of clathrin assembly and curvature. Dynamin recruitment in the end shows the scission of the coated pit. Constant area model for membrane bending observed by pol-TIRF (right panel). Clathrin signal plateaus prior to the start of P/S signal indicating clathrin assembly began as a flat sheet and subsequently remodeled into a vesicle. Dynamin recruitment in the end shows the scission of the coated pit. Reproduced under the terms of the CC BY 4.0 license.[19] Copyright 2018, The Authors, published by Springer Nature. c) Phase diagram of predicted budding state as a function of the scaled membrane tension and scaled clathrin polymerization energy. Four possible states of a single bud are considered in the model: bare membrane with no clathrin binding, shallow membrane with partial budding, hemispherical membrane with partial budding, and spherical membrane with full budding. Reproduced under the terms of the CC BY 4.0 license.[34] Copyright 2015, Nature Publishing Group. d) Transmission electron microscopy images of clathrin buds and flat coats (pointed by blue arrows) under normal condition and osmotic shock (scale bar: 100 nm). Reproduced under the terms of the CC BY 4.0 license.[12] Copyright 2018, The Authors, published by Springer Nature. e) The proportion of flat and domed structures in normal and osmotic shock conditions. An increase in membrane tension by hypo-osmotic shock increases the proportion of flat assemblies. The predicted proportion of flat and domed structure is shown based on the constant area model. Reproduced under the terms of the CC BY 4.0 license.[12] Copyright 2018, The Authors, published by Springer Nature.

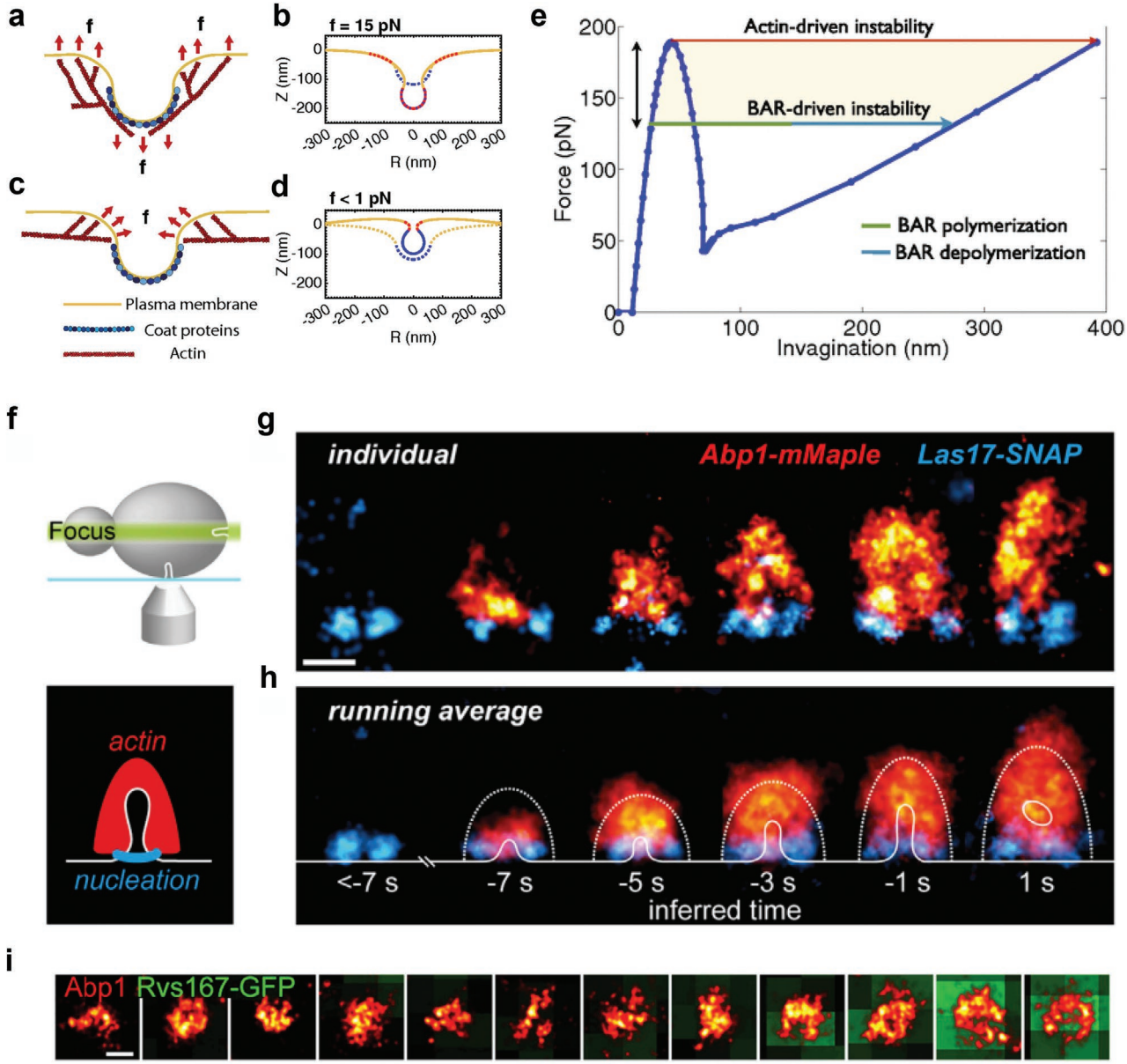

Figure 4. Experimental confirmation of U to Ω transition of clathrin-coated pits (CCPs) with the aid of actin. a) Schematic depicting actin polymerization at the base of a CCP with the network attached to the coat, causing a net inward force on the bud. b) At constant coat area and spontaneous curvature, force (red dash) of actin polymerization adjacent to the coat drives transition of U-shaped pit (dashed line) to Ω-shaped pit (solid line). The final applied inward force on the bud was $f = 15$ pN. c) Schematic depicting actin assembly at the neck of coated pit directly providing a constricting force. d) A constricting force (red dash) of actin polymerization adjacent to the neck of the coat drives transition of U-shaped pit (dashed line) to Ω-shaped pit (solid line). The final applied constriction force on the bud was $f < 1$ pN. Reproduced with permission.[29] Copyright 2017, Proceedings of National Academy of Sciences. e) Synchronous roles of actin and BAR proteins in forming membrane invagination. In the presence of BAR scaffold, a reduced dependence on actin force is required due to a stronger squeezing effect of the BAR scaffold. In the absence of BAR proteins, a tension-dependent critical actin force is needed to induce U to Ω-shaped transition. Reproduced with permission.[30] Copyright 2015, Proceedings of National Academy of Sciences. f) Schematic of dual-color side view super-resolution images (top panel). The localization of actin and actin nucleating proteins (Wiskott–Aldrich syndrome protein (WASp): Las17) in CCPs of yeasts (bottom panel). Reproduced under the terms of the CC BY 4.0 license.[95] Copyright 2018, The Authors, published by Cell Press. g) Dual-color side-view super-resolution images of Las17-SNAP and Abp1-mMaple at individual endocytic sites. h) Running-window averages of Las17 and Abp1 at endocytic sites with overlay of average outer boundaries of the actin network (dotted lines), and average plasma membrane profiles (solid line) (scale bar: 100 nm). Images (g) and (h) show the transition of CCPs from U shape to Ω shape mediated by actin polymerization initiating at the neck of the CCP. Reproduced under the terms of the CC BY 4.0 license.[95] Copyright 2018, The Authors, published by Cell Press. i) Actin binding protein 1 (Abp1) imaged by super-resolution imaging is overlaid on diffraction-limited Rvs167-GFP (BAR protein) in yeast showing the aforementioned synchronous effect for vesicle scission in yeast cells. Reproduced under the terms of the CC BY 4.0.[95] Copyright 2018, The Authors, published by Cell Press.

pits called caveolae.[97] Caveolae are closely associated with actin stress fibers and are internalized in response to various mechanical and chemical stimuli.[28,98] Filamin A anchors caveolae to the plasma membrane by linking them to the actin fibers. Loss of cell adhesion induces rapid internalization and trafficking of caveolae to perinuclear compartments,[99] specifically to recycling endosomes. This internalization is mediated by the loss of linkage between caveolae and actin fibers due to the rapid protein kinase Cα-mediated phosphorylation of filamin A.[100]

Cells respond to increasing membrane tension by flattening or disassembling of caveolae.[101–103] Muscle cells utilize caveolae flattening to protect themselves from membrane rupture due to high tensions.[103] The enhanced membrane fragility in myotubes of muscular dystrophic patients has been attributed to the absence of caveolae reserve in their muscle cells.[103] Similar to individual caveolae, clusters of caveolae known as caveolar rosettes are stabilized by low tension and destabilized by high tension (Figure 2a).[104] It has been shown that plasma membrane wounds induce lysosomal exocytosis and subsequent caveolar rosette formation to seal the membrane.[105] On the other hand, actin fiber anchorage of caveolae inhibits the formation of caveolar rosettes.[106] In response to mechanical stress, cells increase the phosphorylation of early growth response-1 (Egr1) transcription factor and thereby inhibiting its suppression of Cav-1 and cavin-1 genes, which in turn upregulate caveolae biogenesis.[107] Given all these, it is widely accepted that caveolae in the plasma membrane act as a buffer system against rapid membrane tension changes either by flattening of caveolae (during tension increase) or forming caveolae rosettes (during tension decrease).[28]

Cav-1 is implicated in the force-induced cytoskeletal reorganization mediated by RhoA[108] and the maturation of contractile smooth muscle cells induced by transforming growth factor TGF-β1.[109] Cav-1 is also associated with focal adhesion turnover via regulation of RhoA.[110] Further, Cav-1-dependent, β1 integrin, and fibronectin endocytosis mediates fibronectin matrix turnover, pointing toward the role of Cav-1 in ECM remodeling.[111] Low shear stress induces Cav-1 clustering in lipid rafts and co-localization of Cav-1 and membrane type 1-matrix metalloproteinase in invadopodia.[112] Cav-1 activation induces PI3K/Akt/mTOR signaling which in turn promotes motility, invadopodia formation, and metastasis of breast cancer cells.[112] Cav-1 also favors cell elongation in 3D cultures and metastasis by enabling Rho and actomyosin-mediated matrix reorganization.[113] Given the tight connection of Cav-1 with several key cell signaling pathways, coupled with the mechanoregulation of caveolae assembly/disassembly by mechanical stresses, caveolae are viewed as key structures for cells to rapidly respond to extreme mechanical stresses and to changes in ECM due to inflammation and other disease conditions.

5. Clathrin- and Caveolin-Independent Endocytosis

Cells use multiple endocytic pathways that do not involve either clathrin coat formation or caveolae formation. These endocytosis modes have a very high capacity to internalize membrane, thereby making them the rapid responders to abrupt mechanical changes in cells.[22,37,114,115] CIE, as these mechanisms are generally known, is further classified based on whether they use dynamin for membrane scission or not. RhoA-mediated endocytosis, fast endophilin-mediated endocytosis (FEME), Shiga toxin-induced tubules, and ARF6-mediated endocytosis are CIEs involving dynamin for mediating membrane scission. Cdc42-dependent endocytosis (clathrin-independent carriers (CLICs)/glycosylphosphatidylinositol-anchored protein (GPI-AP)-enriched compartments (GEECs) pathway or CG pathway) and flotillin-mediated endocytosis are CIEs that do not use dynamin-mediated scission.[116] One of the major CIE pathway, the CG pathway, has been suggested to be involved in the fast response to membrane tension decrease due to its rapid rate of membrane internalization.[115,117] The surface area-to-volume measurement suggests that the CG pathway can turn over the entire plasma membrane of fibroblasts in 12 min.[117,118] This fast membrane recycling by CG pathway coupled with rapid exocytosis is utilized by fibroblasts to regulate membrane area during spreading.[119] Inhibition of the CG pathway was also shown to reduce membrane tension.[115] Vinculin is shown to mediate the membrane tension response of CG pathway by controlling guanine-nucleotide exchange factor GBF1 in the plasma membrane.[115] Inverted BAR protein IRSp53 enables the formation of tubules in the CG pathway by reducing the force needed to sustain tubules.[120] The activity of IRSp53 to enables tubule formation and to aid membrane scission in the CG pathway is dependent on its density and membrane tension.[121]

Ca^{2+}-dependent endocytosis is involved in rapid sealing of microbial-toxin-induced membrane rupture by internalizing lesions from the plasma membrane.[122] Neuronal synapses use actin and dynamin-mediated ultrafast CIE for recycling synaptic vesicles.[27] Recycling synaptic vesicles is necessary to remove excess membrane from the plasma membrane to maintain optimal tension needed for synaptic vesicle fusion.[27,123] In yeast cells, inhibition of TORC2 controls CIE pathways by modulating membrane tension.[124] Elevated membrane tension upon TORC2 inhibition inhibits the binding of adaptor proteins Sla2 and Ent1 to actin cytoskeleton as well as hinders the recruitment of Rvs167, a N-BAR protein involved in vesicle fission, to endocytic sites, leading to the downregulation of endocytosis in yeast. Altogether, these findings point to the vital role of CIE pathways in rapid reorganization of the plasma membrane in response to physical stresses and membrane ruptures.[125]

6. Macropinocytosis

Macropinocytosis involves nonspecific uptake of extracellular materials via membrane protrusions driven by actin polymerization. The protrusive structures fuse with the basal membrane forming a vesicle of 0.2–0.5 μm in size.[126] Membrane ruffling is heavily associated with the initiation of macropinocytosis. Peterson et al. showed that lipid raft disruptions caused by mechanical or kinetic factors can lead to the activation of phospholipase D2 (PLD2), which is involved in endocytosis and actin polymerization.[127–129] Subsequently,

Loh et al. showed that an acute drop in membrane tension by osmotic shock activated PLD2, which in turn led to phosphatidic acid (PA) production, and F-actin and PIP_2-enriched membrane ruffling in myoblasts. They identified that F-actin and PIP_2-mediated ruffling initiate macropinocytosis.[130] Further, mechanical stretching of muscle cells led to PA-enriched macropinosomes, which act as a platform for mTOR recruitment and activation.[131] Macropinocytosis has been identified as the preferential route of uptake for soft particles like hydrogel-based nanoparticles.[132,133] Aspect ratio of the cargo has also been shown to play an important role in macropinocytosis. Mesoporous silica nanoparticle with an aspect ratio of 2.1–2.5 were preferentially internalized via small GTPase-dependent macropinocytosis compared to nanoparticles with a higher or smaller aspect ratio.[134]

7. Phagocytosis

Phagocytosis involves ingestion of large particles like bacteria into phagosomes for lysosome-based degradation. Phagocytosis involves extensive mechanosensing, membrane and cytoskeletal remodeling, to "search and destroy" pathogens.[5] This remodeling is a two-phase process depending on the membrane tension and other mechanical characteristics of the cell. In the first phase, polymerization of actin pushes the membrane to extend pseudopods. The second phase is initiated once the membrane reservoirs are depleted causing the membrane tension to increase. This membrane tension increase alters activity of small Rho GTPase Rac1, and 3′-phosphoinositide and cytoskeletal organization. Further, it activates exocytosis of GPI-anchored protein-containing vesicles to replenish membrane area that is necessary to carry out phagocytosis of large particles.[36]

Controlling cell shape modulates proinflammatory (M1) versus prohealing (M2) activation of macrophages. Induction of macrophage elongation by confinement in high aspect ratio microcontact-printed islands resulted in polarization toward an M2 phenotype. This confinement upregulated the effect of M2-inducing cytokines while downregulating the effect of M1-inducing cytokines.[135] Preventing cell spreading by spatially confining macrophages on micropatterned islands, circular 3D microwells or cell crowding reduces their bacteria uptake and cytokine secretion.[47] This may be due to reduced transcriptional activity of M1 macrophage that is regulated by actin and myocardin-related transcription factor A (MRTF-A) as a result of area confinement.[47] Further, macrophages were unable to phagocytose filament-formed *E. coli* that have high aspect ratio, as such structures presented limited access of bacteria poles for macrophages to initiate phagocytosis.[63] Beningo et al. showed that Fc-mediated phagocytosis is regulated by the mechanical properties of its target. By microinjecting constitutively active Rac1, phagocytosis of softer particles by macrophages could be activated.[136] Bakalar et al. showed that antigen height mediates the phagocytosis of engineered and tumor-specific antigens.[137] Phagocytosis was severely inhibited by antigens that created a separation of more than 10 nm between antibodies and target surface.[137] The ability for macrophages to detect variations in ECM stiffness associated with tissue inflammation is necessary for their phagocytic response. Scheraga et al. showed that a mechanosensitive ion channel transient receptor potential vanilloid 4 (TRPV4), triggered by changes in ECM stiffness due to inflamed or fibrotic lung, mediates lipopolysaccharide-stimulated murine macrophage phagocytosis.[49] Bacterial pathogen-associated molecular pattern molecules (PAMPs), cytokines (IFNγ), substrate rigidity, and stretch via actin polymerization and small Rho GTPase activity can control macrophage phagocytosis independently. This suggests a coordinated mechanism to increase macrophage phagocytosis in disease states like pneumonia, which is associated with an increase in tissue rigidity and production of PAMPs or inflammatory cytokines.[48] This mechanism likely plays an important role in regulating macrophage activity during pulmonary infection and fibrosis.[49]

Table 1 highlights some of the components in the "mechanome" of endocytosis from different endocytic pathways, and what their stimuli and mechanoresponses are.

8. Conclusion and Perspective

Endocytosis has been studied in detail over the past half century.[4] However, a holistic view into the mechanoregulation of endocytic process is only beginning to gain traction in the last decade. Advances in light and electron microscopy with high spatiotemporal resolution and micromechanical manipulation of cells have together pushed the technical capabilities to dissect the mechanoregulation of endocytosis. The survey of some recent studies reveals endocytosis as a process heavily regulated by the mechanical properties of plasma membrane, ECM, and cargo. Emerging studies are beginning to quantify mechanochemical responses of endocytic proteins during endocytosis. New endocytic pathways, such as FEME and ultrafast endocytosis, may also be mechanisms that cells utilize to counter extreme changes in mechanical properties of cells and their surroundings. Given the diverse mechanisms of endocytosis, an important question for future research is to ask whether different endocytic pathways are differentially regulated by mechanical stimuli. From what is currently known, it appears that an increase in membrane tension inhibits all endocytosis. It would be illuminating to monitor two endocytic pathways simultaneously when mechanically perturbed. Further, new knowledge on noncoated mechanosensitive endocytic processes is poised to challenge the existing notions of protein specific membrane bending mechanisms. Alternate mechanisms for membrane bending like steric repulsion by protein crowding, cargo clustering will gain more prominence as a key mechanism for membrane sculpting. The physiological impact of mechanically regulated endocytosis will also be of significant interest. In particular, many of the endocytic pathways have direct connections to cell signaling pathways. Thus, it is conceivable that part of the mechanotransduction pathway is related to the effect of mechanical stimuli on endocytosis. The plethora of mechanosensitive endocytic processes available at the disposal of cells may point toward an evolutionarily conserved role of endocytosis as a key mechanoregulator.

Organisms undergo and respond to a wide range of mechanical stimuli. Many of the disease states are accompanied by changes in mechanical properties of cells and tissues. The ubiquitous nature of endocytosis and the diverse range of mechanical stimuli in higher organisms pose a great challenge in delineating their co-dependences across different organisms and different biological processes. Current understanding of the mechanics of endocytosis is obtained exclusively from single cell studies performed on 2D cultures. However, mechanical stimuli and endocytosis play more complex role in multicellular processes like embryo development, angiogenesis, and neural plasticity. Exciting new advancements in microscopy like lattice light sheet microscopy will be instrumental in imaging endocytosis in living organisms beyond the imaging depth of conventional microscopy. Advancements in imaging of endocytic processes in higher-order organisms also call for a greater

Table 1. Mechanome of endocytosis. Important mechanosensitive proteins involved in different endocytosis pathways. A brief description of mechanical stimuli and response of each protein to a particular stimulus is provided.

Endocytosis process	Associated protein or protein complex	Mechanical stimuli	Response to mechanical stimuli	Refs.
Clathrin-mediated endocytosis	Clathrin	Membrane tension	Reduction in recruitment.	[25]
	Actin	Membrane tension	Actin polymerization enables transition of open CCP to closed CCP prior to scission at high tension.	[8]
	ENTH domain proteins	Membrane tension	H_0 helix insertion into membrane causes tubule formation at low lateral tension, whereas it reduces membrane rigidity at higher membrane tension.	[41]
	N-BAR proteins	Membrane tension	Oligomerization of bar proteins and their interaction with membrane is inhibited by tension.	[79]
Caveolae-mediated endocytosis	Cav-1	Low shear stress	Cav-1 clustering in lipid rafts and activation of PI3K/Akt/mTOR signaling.	[112]
	Cav-1 and cavin-1	Membrane stretch	Reduction in Cav-1 cavin-1 interaction by membrane stretch causes caveolae disassembly. Cavin-1 becomes cytosolic.	[103]
	Filamin A	Loss of cell adhesion	Phosphorylation of filamin A causes loss of linkage between caveolae and actin fibers.	[100]
Clathrin/caveolae-independent endocytosis	GPI-anchored proteins	Membrane tension	Drop in tension upregulates CLIC/GEEC pathway and uptake of GPI-anchored protein.	[115,118]
	Vinculin	Membrane tension	Inhibit CLIC/GEEC pathway endocytosis to reduce tension.	[115]
	TORC2	Membrane tension	Drop in tension causes clustering of TORC2 to PtdIns(4,5)P2-enriched PM domains and induces CIE.	[124]
Macropinocytosis	Rac1 and CDC42	Aspect ratio of cargo	Differentially uptake NPs of aspect ratio 2.1–2.5, by forming filopodia with activation of the actin cytoskeleton.	[134]
	Phosphatidic acid	Membrane stretching	Enrichment of PA in macropinosomes, which act as a platform for mTOR recruitment and activation.	[131]
	PLD2	Membrane tension	Activation of PLD2 leads to phosphatidic acid (PA) production, and F-actin and PIP2-enriched membrane ruffling in myoblasts.	[130]
Phagocytosis	Rac1	Substrate stiffness and membrane tension	Control actin reorganization for cup formation and activate phagocytosis of softer particles.	[48,136]
	Cdc42	Substrate stiffness	Promote actin organization and increase cell elasticity	[48]
	Myocardin-related transcription factor-A (MRTF-A)	Area confinement	Downregulation leads to reduction in M1 macrophage transcription.	[47]
	Transient receptor potential vanilloid 4 (TRPV4) ion channel	Substrate stiffness	Extracellular matrix stiffness in the range of inflamed/fibrotic lung promotes TRPV4 activity leading to anti-inflammatory phenotypic change and increase in phagocytic activity.	[49]

need in developing automated methods that can simultaneously detect, track, and analyze thousands of in vivo endocytic events in the midst of interference from motion of organisms, background noise from tissues, and other artifacts. Uncovering the interdependence of mechanical stimuli and endocytic pathways in these contexts will require a combination of sophisticated imaging approaches, powerful analytic techniques, and novel tissue manipulation methods.

Acknowledgements

J.G.J. and A.P.L. were supported by NSF-BMMB 1561794.

Conflict of Interest

The authors declare no conflict of interest.

Keywords

clathrin-mediated endocytosis, endocytosis pathways, mechanobiology, mechanotargeting, mechanotransduction

Received: November 23, 2019
Revised: March 2, 2020
Published online: March 24, 2020

[1] M. Kaksonen, A. A. Roux, *Nat. Rev. Mol. Cell Biol.* **2018**, *19*, 313.
[2] M. C. Jones, P. T. Caswell, J. C. Norman, *Curr. Opin. Cell Biol.* **2006**, *18*, 549.
[3] M. Fürthauer, M. González-Gaitán, *Cell Cycle* **2009**, *8*, 3311.
[4] H. T. McMahon, E. Boucrot, *Nat. Rev. Mol. Cell Biol.* **2011**, *12*, 517.
[5] N. Jain, J. Moeller, V. Vogel, *Annu. Rev. Biomed. Eng.* **2019**, *21*, 267.
[6] J. J. Thottacherry, M. Sathe, C. Prabhakara, S. Mayor, *Annu. Rev. Cell Dev. Biol.* **2019**, *35*, 55.
[7] M. M. Lacy, R. Ma, N. G. Ravindra, J. Berro, *FEBS Lett.* **2018**, *592*, 3586.
[8] S. Boulant, C. Kural, J.-C. C. Zeeh, F. Ubelmann, T. Kirchhausen, *Nat. Cell Biol.* **2011**, *13*, 1124.
[9] G. J. Doherty, H. T. McMahon, *Annu. Rev. Biochem.* **2009**, *78*, 857.
[10] J. Zhao, M. H. Stenzel, *Polym. Chem.* **2018**, *9*, 259.
[11] K. A. Sochacki, J. W. Taraska, *Trends Cell Biol.* **2019**, *29*, 241.
[12] D. Bucher, F. Frey, K. A. Sochacki, S. Kummer, J.-P. Bergeest, W. J. Godinez, H.-G. Kräusslich, K. Rohr, J. W. Taraska, U. S. Schwarz, S. Boulant, *Nat. Commun.* **2018**, *9*, 1109.
[13] A. P. Liu, O. Chaudhuri, S. H. Parekh, *Integr. Biol.* **2017**, *9*, 383.
[14] M. Eisenstein, *Nature* **2017**, *544*, 255.
[15] A. Diz-Muñoz, O. D. Weiner, D. A. Fletcher, *Nat. Phys.* **2018**, *14*, 648.
[16] J. P. Ferguson, N. M. Willy, S. P. Heidotting, S. D. Huber, M. J. Webber, C. Kural, *J. Cell Biol.* **2016**, *214*, 347.
[17] F. Aguet, C. N. Antonescu, M. Mettlen, S. L. Schmid, G. Danuser, *Dev. Cell* **2013**, *26*, 279.
[18] N. M. Willy, J. P. Ferguson, S. D. Huber, S. P. Heidotting, E. Aygün, S. A. Wurm, E. Johnston-Halperin, M. G. Poirier, C. Kural, *Mol. Biol. Cell* **2017**, *28*, 3480.
[19] B. L. Scott, K. A. Sochacki, S. T. Low-Nam, E. M. Bailey, Q. A. Luu, A. Hor, A. M. Dickey, S. Smith, J. G. Kerkvliet, J. W. Taraska, A. D. Hoppe, *Nat. Commun.* **2018**, *9*, 419.
[20] J. C. Stachowiak, E. M. Schmid, C. J. Ryan, H. S. Ann, D. Y. Sasaki, M. B. Sherman, P. L. Geissler, D. A. Fletcher, C. C. Hayden, *Nat. Cell Biol.* **2012**, *14*, 944.
[21] D. J. Busch, J. R. Houser, C. C. Hayden, M. B. Sherman, E. M. Lafer, J. C. Stachowiak, *Nat. Commun.* **2015**, *6*, 7875.
[22] N. C. Gauthier, T. A. Masters, M. P. Sheetz, *Trends Cell Biol.* **2012**, *22*, 527.
[23] J. Dai, M. P. Sheetz, *Cold Spring Harbor Symp. Quant. Biol.* **1995**, *60*, 567.
[24] O. L. Mooren, B. J. Galletta, J. A. Cooper, *Annu. Rev. Biochem.* **2012**, *81*, 661.
[25] X. Tan, J. Heureaux, A. P. Liu, *Integr. Biol.* **2015**, *7*, 1033.
[26] G. Apodaca, *Am. J. Physiol.: Renal Physiol.* **2002**, *282*, F179.
[27] S. Watanabe, E. Boucrot, *Curr. Opin. Cell Biol.* **2017**, *47*, 64.
[28] A. Echarri, M. A. Del Pozo, *J. Cell Sci.* **2015**, *128*, 2747.
[29] J. E. Hassinger, G. Oster, D. G. Drubin, P. Rangamani, *Proc. Natl. Acad. Sci. USA* **2017**, *114*, E1118.
[30] N. Walani, J. Torres, A. Agrawal, *Proc. Natl. Acad. Sci. USA* **2015**, *2015*, 201418491.
[31] J. P. Ferguson, S. D. Huber, N. M. Willy, E. Aygün, S. Goker, T. Atabey, C. Kural, *J. Cell Sci.* **2017**, *130*, 3631.
[32] F. Baschieri, S. Dayot, N. Elkhatib, N. Ly, A. Capmany, K. Schauer, T. Betz, D. M. Vignjevic, R. Poincloux, G. Montagnac, *Nat. Commun.* **2018**, *9*, 3825.
[33] E. Irajizad, N. Walani, S. L. Veatch, A. P. Liu, A. Agrawal, *Soft Matter* **2017**, *13*, 1455.
[34] M. Saleem, S. Morlot, A. Hohendahl, J. Manzi, M. Lenz, A. Roux, *Nat. Commun.* **2015**, *6*, 6249.
[35] Z. Shi, T. Baumgart, *Nat. Commun.* **2015**, *6*, 5974.
[36] T. A. Masters, B. Pontes, V. Viasnoff, Y. Li, N. C. Gauthier, *Proc. Natl. Acad. Sci. USA* **2013**, *110*, 11875.
[37] J. J. Thottacherry, A. J. Kosmalska, S. Pradhan, P. P. Singh, X. Trepat, R. Vishwakarma, P. Pullarkat, P. Roca-Cusachs, S. Mayor, *Biophys. J.* **2019**, *116*, 92a.
[38] J. C. Stachowiak, F. M. Brodsky, E. A. Miller, *Nat. Cell Biol.* **2013**, *15*, 1019.
[39] R. Dimova, *Adv. Colloid Interface Sci.* **2014**, *208*, 225.
[40] M. Pinot, S. Vanni, S. Pagnotta, S. Lacas-Gervais, L.-A. Payet, T. Ferreira, R. Gautier, B. Goud, B. Antonny, H. Barelli, *Science* **2014**, *345*, 693.
[41] M. Gleisner, B. Kroppen, C. Fricke, N. Teske, T.-T. Kliesch, A. Janshoff, M. Meinecke, C. Steinem, *J. Biol. Chem.* **2016**, *291*, 19953.
[42] A. Zemel, A. Ben-Shaul, S. May, *J. Phys. Chem. B* **2008**, *112*, 6988.
[43] A. Čopič, C. F. Latham, M. A. Horlbeck, J. G. D'Arcangelo, E. A. Miller, *Science* **2012**, *335*, 1359.
[44] L. Johannes, C. Wunder, P. Bassereau, *Cold Spring Harbor Perspect. Biol.* **2014**, *6*, a016741.
[45] S. Morlot, V. Galli, M. Klein, N. Chiaruttini, J. Manzi, F. Humbert, L. Dinis, M. Lenz, G. Cappello, A. Roux, *Cell* **2012**, *151*, 619.
[46] D. Missirlis, *PLoS One* **2014**, *9*, e96548.
[47] N. Jain, V. Vogel, *Nat. Mater.* **2018**, *17*, 1134.
[48] N. R. Patel, M. Bole, C. Chen, C. C. Hardin, A. T. Kho, J. Mih, L. Deng, J. Butler, D. Tschumperlin, J. J. Fredberg, R. Krishnan, H. Koziel, *PLoS One* **2012**, *7*, e41024.
[49] R. G. Scheraga, S. Abraham, K. A. Niese, B. D. Southern, L. M. Grove, R. D. Hite, C. McDonald, T. A. Hamilton, M. A. Olman, *J. Immunol.* **2016**, *196*, 428.
[50] F. Bordeleau, B. N. Mason, E. M. Lollis, M. Mazzola, M. R. Zanotelli, S. Somasegar, J. P. Califano, C. Montague, D. J. LaValley, J. Huynh, N. Mencia-Trinchant, Y. L. N. Abril, D. C. Hassane, L. J. Bonassar, J. T. Butcher, R. S. Weiss, C. A. Reinhart-King, *Proc. Natl. Acad. Sci. USA* **2017**, *114*, 492.
[51] D. J. LaValley, M. R. Zanotelli, F. Bordeleau, W. Wang, S. C. Schwager, C. A. Reinhart-King, *Convergent Sci. Phys. Oncol.* **2017**, *3*, 044001.

[52] J. Li, H. Chen, Y. Xu, J. Hu, F. Q. Xie, C. Yang, *J. Biomech.* **2016**, *49*, 2644.
[53] E. M. Batchelder, D. Yarar, *Mol. Biol. Cell* **2010**, *21*, 3070.
[54] P. Maupin, T. D. Pollard, *J. Cell Biol.* **1983**, *96*, 51.
[55] J. Heuser, *J. Cell Biol.* **1989**, *108*, 401.
[56] C. Huang, P. J. Butler, S. Tong, H. S. Muddana, G. Bao, S. Zhang, *Nano Lett.* **2013**, *13*, 1611.
[57] A. C. Anselmo, S. Mitragotri, *Adv. Drug Delivery Rev.* **2017**, *108*, 51.
[58] A. C. Anselmo, M. Zhang, S. Kumar, D. R. Vogus, S. Menegatti, M. E. Helgeson, S. Mitragotri, *ACS Nano* **2015**, *9*, 3169.
[59] F. Lu, S.-H. Wu, Y. Hung, C.-Y. Mou, *Small* **2009**, *5*, 1408.
[60] B. D. Chithrani, A. A. Ghazani, W. C. W. Chan, *Nano Lett.* **2006**, *6*, 662.
[61] S. Dasgupta, T. Auth, G. Gompper, *Nano Lett.* **2014**, *14*, 687.
[62] A. A. Brakhage, S. Bruns, A. Thywissen, P. F. Zipfel, J. Behnsen, *Curr. Opin. Microbiol.* **2010**, *13*, 409.
[63] J. Möller, T. Luehmann, H. Hall, V. Vogel, *Nano Lett.* **2012**, *12*, 2901.
[64] J. Sun, L. Zhang, J. Wang, Q. Feng, D. Liu, Q. Yin, D. Xu, Y. Wei, B. Ding, X. Shi, X. Jiang, *Adv. Mater.* **2015**, *27*, 1402.
[65] T. M. Kruger, B. E. Givens, T. I. Lansakara, K. J. Bell, H. Mohapatra, A. K. Salem, A. V. Tivanski, L. L. Stevens, *ACS Appl. Bio Mater.* **2018**, *1*, 1254.
[66] Q. Wei, C. Huang, Y. Zhang, T. Zhao, P. Zhao, P. Butler, S. Zhang, *Adv. Mater.* **2018**, *30*, 1707464.
[67] S. Zhang, H. Gao, G. Bao, *ACS Nano* **2015**, *9*, 8655.
[68] S. Zhang, J. Li, G. Lykotrafitis, G. Bao, S. Suresh, *Adv. Mater.* **2009**, *21*, 419.
[69] S. D. Conner, S. L. Schmid, *Nature* **2003**, *422*, 37.
[70] W. M. Henne, E. Boucrot, M. Meinecke, E. Evergren, Y. Vallis, R. Mittal, H. T. McMahon, *Science* **2010**, *328*, 1281.
[71] E. Cocucci, F. Aguet, S. Boulant, T. Kirchhausen, *Cell* **2012**, *150*, 495.
[72] M. Ehrlich, W. Boll, A. Van Oijen, R. Hariharan, K. Chandran, M. L. Nibert, T. Kirchhausen, *Cell* **2004**, *118*, 591.
[73] D. Nunez, C. Antonescu, M. Mettlen, A. Liu, S. L. Schmid, D. Loerke, G. Danuser, *Traffic* **2011**, *12*, 1868.
[74] L. Ma, P. K. Umasankar, A. G. Wrobel, A. Lymar, A. J. McCoy, S. S. Holkar, A. Jha, T. Pradhan-Sundd, S. C. Watkins, D. J. Owen, L. M. Traub, *Dev. Cell* **2016**, *37*, 428.
[75] L. Wang, A. Johnson, M. Hanna, A. Audhya, *Mol. Biol. Cell* **2016**, *27*, 2675.
[76] A. P. Liu, D. Loerke, S. L. Schmid, G. Danuser, *Biophys. J.* **2009**, *97*, 1038.
[77] X. Tan, M. Luo, A. P. Liu, *Heliyon* **2018**, *4*, e00819.
[78] W. Zhao, L. Hanson, H. Y. Lou, M. Akamatsu, P. D. Chowdary, F. Santoro, J. R. Marks, A. Grassart, D. G. Drubin, Y. Cui, B. Cui, *Nat. Nanotechnol.* **2017**, *12*, 750.
[79] M. Simunovic, G. A. Voth, *Nat. Commun.* **2015**, *6*, 7219.
[80] A. Diz-Muñoz, D. A. Fletcher, O. D. Weiner, *Trends Cell Biol.* **2013**, *23*, 47.
[81] I. K. Jarsch, F. Daste, J. L. Gallop, *J. Cell Biol.* **2016**, *214*, 375.
[82] C.-L. Lai, C. C. Jao, E. Lyman, J. L. Gallop, B. J. Peter, H. T. McMahon, R. Langen, G. A. Voth, *J. Mol. Biol.* **2012**, *423*, 800.
[83] J. B. Hutchison, A. P. K. K. K. Mudiyanselage, R. M. Weis, A. D. Dinsmore, *Soft Matter* **2016**, *12*, 2465.
[84] H. Cui, E. Lyman, G. A. Voth, *Biophys. J.* **2011**, *100*, 1271.
[85] G. Drin, B. Antonny, *FEBS Lett.* **2010**, *584*, 1840.
[86] J. C. Stachowiak, C. C. Hayden, D. Y. Sasaki, *Proc. Natl. Acad. Sci. USA* **2010**, *107*, 7781.
[87] H. Y. Naim, *J. Cell Biol.* **1995**, *129*, 1241.
[88] S. Saffarian, E. Cocucci, T. Kirchhausen, *PLoS Biol.* **2009**, *7*, e1000191.
[89] N. Cordella, T. J. Lampo, S. Mehraeen, A. J. Spakowitz, *Biophys. J.* **2014**, *106*, 1476.
[90] O. Avinoam, M. Schorb, C. J. Beese, J. A. G. Briggs, M. Kaksonen, *Science* **2015**, *348*, 1369.
[91] S. E. Miller, S. Mathiasen, N. A. Bright, F. Pierre, B. T. Kelly, N. Kladt, A. Schauss, C. J. Merrifield, D. Stamou, S. Höning, D. J. Owen, *Dev. Cell* **2015**, *33*, 163.
[92] A. Grassart, A. T. Cheng, S. H. Hong, F. Zhang, N. Zenzer, Y. Feng, D. M. Briner, G. D. Davis, D. Malkov, D. G. Drubin, *J. Cell Biol.* **2014**, *205*, 721.
[93] A. Henry, J. Hislop, J. Grove, K. Thorn, M. Marsh, M. von Zastrow, *Dev. Cell* **2012**, *23*, 519.
[94] C. Chen, X. Zhuang, *Proc. Natl. Acad. Sci. USA* **2008**, *105*, 11790.
[95] M. Mund, J. A. van der Beek, J. Deschamps, S. Dmitrieff, P. Hoess, J. L. Monster, A. Picco, F. Nédélec, M. Kaksonen, J. Ries, *Cell* **2018**, *174*, 884.
[96] M. Simunovic, J.-B. Manneville, H.-F. Renard, E. Evergren, K. Raghunathan, D. Bhatia, A. K. Kenworthy, G. A. Voth, J. Prost, H. T. McMahon, L. Johannes, P. Bassereau, A. Callan-Jones, *Cell* **2017**, *170*, 172.
[97] R. G. Parton, K. Simons, *Nat. Rev. Mol. Cell Biol.* **2007**, *8*, 185.
[98] T. Richter, M. Floetenmeyer, C. Ferguson, J. Galea, J. Goh, M. R. Lindsay, G. P. Morgan, B. J. Marsh, R. G. Parton, *Traffic* **2008**, *9*, 893.
[99] M. A. del Pozo, N. Balasubramanian, N. B. Alderson, W. B. Kiosses, A. Grande-García, R. G. W. Anderson, M. A. Schwartz, *Nat. Cell Biol.* **2005**, *7*, 901.
[100] O. Muriel, A. Echarri, C. Hellriegel, D. M. Pavon, L. Beccari, M. A. Del Pozo, *J. Cell Sci.* **2011**, *124*, 2763.
[101] L. Kozera, E. White, S. Calaghan, *PLoS One* **2009**, *4*, e8312.
[102] O. L. Gervasio, W. D. Phillips, L. Cole, D. G. Allen, *J. Cell Sci.* **2011**, *124*, 3581.
[103] B. Sinha, D. Köster, R. Ruez, P. Gonnord, M. Bastiani, D. Abankwa, R. V. Stan, G. Butler-Browne, B. Vedie, L. Johannes, N. Morone, R. G. Parton, G. G. Raposo, P. Sens, C. Lamaze, P. Nassoy, *Cell* **2011**, *144*, 402.
[104] G. Golani, N. Ariotti, R. G. Parton, M. M. Kozlov, *Dev. Cell* **2019**, *48*, 523.
[105] M. Corrotte, P. E. Almeida, C. Tam, T. Castro-Gomes, M. C. Fernandes, B. A. Millis, M. Cortez, H. Miller, W. Song, T. K. Maugel, N. W. Andrews, *eLife* **2013**, *2*, e00926.
[106] D. I. Mundy, *J. Cell Sci.* **2002**, *115*, 4327.
[107] B. Joshi, M. Bastiani, S. S. Strugnell, C. Boscher, R. G. Parton, I. R. Nabi, *J. Cell Biol.* **2012**, *199*, 425.
[108] F. Peng, D. Wu, A. J. Ingram, B. Zhang, B. Gao, J. C. Krepinsky, *J. Am. Soc. Nephrol.* **2007**, *18*, 189.
[109] R. Gosens, G. L. Stelmack, G. Dueck, M. M. Mutawe, M. Hinton, K. D. McNeill, A. Paulson, S. Dakshinamurti, W. T. Gerthoffer, J. A. Thliveris, H. Unruh, J. Zaagsma, A. J. Halayko, *Am. J. Physiol.: Lung Cell. Mol. Physiol.* **2007**, *293*, L1406.
[110] H. Urra, V. A. Torres, R. J. Ortiz, L. Lobos, M. I. Díaz, N. Díaz, S. Härtel, L. Leyton, A. F. G. Quest, *PLoS One* **2012**, *7*, e33085.
[111] F. Shi, J. Sottile, *J. Cell Sci.* **2008**, *121*, 2360.
[112] H. Yang, L. Guan, S. Li, Y. Jiang, N. Xiong, L. Li, C. Wu, H. Zeng, Y. Liu, *Oncotarget* **2016**, *7*, 16227.
[113] J. Goetz, S. Minguet, I. Navarro-Lérida, J. Lazcano, R. Samaniego, E. Calvo, M. Tello, T. Osteso-Ibáñez, T. Pellinen, A. Echarri, A. Cerezo, A. P. Klein-Szanto, R. Garcia, P. Keely, P. Sánchez-Mateos, E. Cukierman, M. Del Pozo, *Cell* **2011**, *146*, 148.
[114] K. Sandvig, S. Pust, T. Skotland, B. van Deurs, *Curr. Opin. Cell Biol.* **2011**, *23*, 413.
[115] J. J. Thottacherry, A. J. Kosmalska, A. Kumar, A. S. Vishen, A. Elosegui-Artola, S. Pradhan, S. Sharma, P. P. Singh, M. C. Guadamillas, N. Chaudhary, R. Vishwakarma, X. Trepat, M. A. del Pozo, R. G. Parton, M. Rao, P. Pullarkat, P. Roca-Cusachs, S. Mayor, *Nat. Commun.* **2018**, *9*, 4217.

[116] K. Sandvig, S. Kavaliauskiene, T. Skotland, *Histochem. Cell Biol.* **2018**, *150*, 107.
[117] M. T. Howes, M. Kirkham, J. Riches, K. Cortese, P. J. Walser, F. Simpson, M. M. Hill, A. Jones, R. Lundmark, M. R. Lindsay, D. J. Hernandez-Deviez, G. Hadzic, A. McCluskey, R. Bashir, L. Liu, P. Pilch, H. McMahon, P. J. Robinson, J. F. Hancock, S. Mayor, R. G. Parton, *J. Cell Biol.* **2010**, *190*, 675.
[118] M. T. Howes, S. Mayor, R. G. Parton, *Curr. Opin. Cell Biol.* **2010**, *22*, 519.
[119] N. C. Gauthier, O. M. Rossier, A. Mathur, J. C. Hone, M. P. Sheetz, *Mol. Biol. Cell* **2009**, *20*, 3261.
[120] C. Prévost, H. Zhao, J. Manzi, E. Lemichez, P. Lappalainen, A. Callan-Jones, P. Bassereau, *Nat. Commun.* **2015**, *6*, 8529.
[121] M. Sathe, G. Muthukrishnan, J. Rae, A. Disanza, M. Thattai, G. Scita, R. G. Parton, S. Mayor, *Nat. Commun.* **2018**, *9*, 1835.
[122] V. Idone, C. Tam, J. W. Goss, D. Toomre, M. Pypaert, N. W. Andrews, *J. Cell Biol.* **2008**, *180*, 905.
[123] L. V. Chernomordik, M. M. Kozlov, *Nat. Struct. Mol. Biol.* **2008**, *15*, 675.
[124] M. Riggi, C. Bourgoint, M. Macchione, S. Matile, R. Loewith, A. Roux, *J. Cell Biol.* **2019**, *218*, 2265.
[125] J. Donaldson, N. Poratschliom, L. Cohen, *Cell. Signalling* **2009**, *21*, 1.
[126] L. Hu, Z. Mao, C. Gao, *J. Mater. Chem.* **2009**, *19*, 3108.
[127] E. N. Petersen, H.-W. Chung, A. Nayebosadri, S. B. Hansen, *Nat. Commun.* **2016**, *7*, 13873.
[128] G. Du, P. Huang, B. T. Liang, M. A. Frohman, *Mol. Biol. Cell* **2004**, *15*, 1024.
[129] Y. Jiang, M. S. Sverdlov, P. T. Toth, L. S. Huang, G. Du, Y. Liu, V. Natarajan, R. D. Minshall, *J. Biol. Chem.* **2016**, *291*, 20729.
[130] J. Loh, M.-C. Chuang, S.-S. Lin, J. Joseph, Y.-A. Su, T.-L. Hsieh, Y.-C. Chang, A. P. Liu, Y.-W. Liu, *J. Cell Sci.* **2019**, *132*, jcs232579.
[131] S.-S. Lin, Y.-W. Liu, *Front. Cell Dev. Biol.* **2019**, *7*, 78.
[132] X. Banquy, F. Suarez, A. Argaw, J.-M. Rabanel, P. Grutter, J.-F. Bouchard, P. Hildgen, S. Giasson, *Soft Matter* **2009**, *5*, 3984.
[133] W. Liu, X. Zhou, Z. Mao, D. Yu, B. Wang, C. Gao, *Soft Matter* **2012**, *8*, 9235.
[134] H. Meng, S. Yang, Z. Li, T. Xia, J. Chen, Z. Ji, H. Zhang, X. Wang, S. Lin, C. Huang, Z. H. Zhou, J. I. Zink, A. E. Nel, *ACS Nano* **2011**, *5*, 4434.
[135] F. Y. McWhorter, T. Wang, P. Nguyen, T. Chung, W. F. Liu, *Proc. Natl. Acad. Sci. USA* **2013**, *110*, 17253.
[136] K. A. Beningo, C.-M. Lo, Y.-L. Wang, *Methods in Cell Biology*, Elsevier, Amsterdam **2002**, pp. 325–339.
[137] M. H. Bakalar, A. M. Joffe, E. M. Schmid, S. Son, M. Podolski, D. A. Fletcher, *Cell* **2018**, *174*, 131.

